Vibrational Edge Modes for Wedges with Arbitrary Interior Angles

S. L. Moss*, A. A. Maradudin*, and S. L. Cunningham†
Department of Physics, University of California, Irvine, California 92664
(Received 12 February 1973)

We present a theory of long-wavelength acoustic phonons localized at the apex of a variable-angle semi-infinite wedge made up of an isotropic cubic elastic medium. Stress-free boundary conditions are incorporated into the calculation by assuming position-dependent elastic constants. The equations of motion are solved numerically by first performing a linear mapping of the wedge into a right-angle wedge, and then expanding each displacement component in a double series of Laguerre functions. When the Cauchy relation is satisfied and when the interior angle of the wedge is between 125° and 180°, the speed of the lowest-frequency edge mode, which is of Γ_1 symmetry, is very nearly equal to the speed of Rayleigh surface waves. For wedge angles less than 100°, the speed of the lowest-frequency edge mode, which is now of Γ_2 symmetry, decreases rapidly with angle and appears to vanish in the limit as the angle approaches 0°. For these acute angles, additional edge modes of Γ_2 symmetry appear with speeds below the Rayleigh value.

I. INTRODUCTION

In a recent paper[1] a theory was presented of acoustic waves which propagate along the edge of a right-angle wedge of a cubic elastic medium, and whose displacement amplitudes decay with increasing distance into the medium from the edge. Such waves were termed vibrational edge modes. For the case of an isotropic elastic medium, whose Lamé constants obey the Poisson condition, the speed of propagation of these modes was found to be very slightly lower than that of Rayleigh surface waves.

In this paper we extend the analysis of Ref. 1 to the study of vibrational edge modes associated with the edge of a cubic elastic wedge of arbitrary interior angle, between 0° and 180°, symmetrically disposed with respect to a (110) plane.

After the work reported in this paper was substantially completed the authors received a preprint of a paper by Lagasse, Mason, and Ash, in which theoretical and experimental results are presented for the speeds of propagation of vibrational edge modes on wedges of Duralumin 17S and PZT4A of varying internal angles.[2] The method of calculation used by these authors, a variational method capable of application to piezoelectric as well as to nonpiezoelectric materials, is somewhat different from that presented in this paper, which at present has been applied only to nonpiezoelectric materials. Consequently, the method developed in this paper for obtaining the displacement field and speed of a vibrational edge mode on a wedge of arbitrary interior angle, which can be applied to situations more complex than those considered here, may have an interest independent of the results obtained by its use. Allowing for the differences in the materials considered, the results we obtain are in agreement with those of Lagasse, Mason, and Ash.

A theory of electrostatic edge modes on a dielectric wedge of arbitrary interior angle has recently been presented.[3]

II. THEORY

The elastic wedge which we study in this paper is defined by the equations

$$x_2 \geq m x_1 , \tag{1a}$$

$$x_1 \geq m x_2 , \tag{1b}$$

$$-\infty \leq x_3 \leq \infty , \tag{1c}$$

with

$$-1 \leq m \leq 1 \tag{2}$$

(see Fig. 1). The internal angle of the wedge is

$$\theta = \tan^{-1}\left(\frac{1-m^2}{2m}\right) , \tag{3}$$

and the wedge is symmetrically situated with respect to the plane $x_1 = x_2$. The choice $m = 0$ ($\theta = \frac{1}{2}\pi$) corresponds to the right-angle wedge studied in Ref. 1; the choice $m = -1$ ($\theta = \pi$) corresponds to a semi-infinite solid bounded by the plane surface $x_2 = -x_1$; the choice $m = 1$ ($\theta = 0$) corresponds to the degenerate case of an infinitely thin wedge, in fact the plane $x_1 = x_2$ for $x_1, x_2 > 0$. Thus, by varying the constant m from $+1$ to -1, the internal angle of the wedge can be varied continuously from 0 to π rad.

The equations of motion for an elastic continuum with position-dependent elastic constants are

$$\rho \ddot{u}_\alpha = \sum_{\beta\mu\nu} \frac{\partial C_{\alpha\beta\mu\nu}}{\partial x_\beta} \frac{\partial u_\mu}{\partial x_\nu} + \sum_{\beta\mu\nu} C_{\alpha\beta\mu\nu} \frac{\partial^2 u_\mu}{\partial x_\beta \partial x_\nu} . \tag{4}$$

In these equations $u_\alpha(\vec{x}, t)$ is the α Cartesian component of the elastic displacement field at the point $\vec{x} = (x_1, x_2, x_3)$ at the time t, and the $\{C_{\alpha\beta\mu\nu}(\vec{x})\}$ are

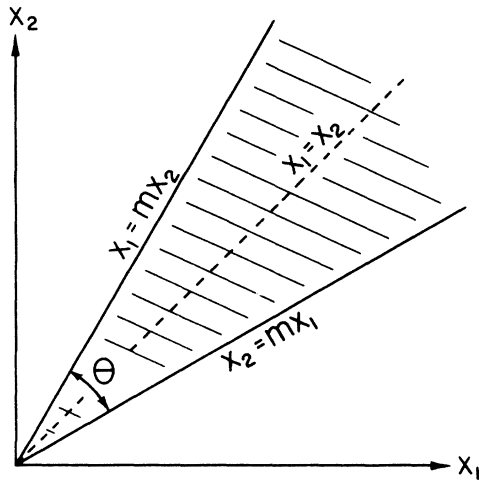

FIG. 1. Configuration of the elastic wedge showing the wedge angle θ and the equations of the bounding surfaces. The wedge is centered on the plane $x_1 = x_2$.

the elastic constants.

The position dependence of the elastic constants of the wedge defined by Eqs. (1)–(2) is given by

$$C_{\alpha\beta\mu\nu}(\vec{x}) = \theta(x_2 - mx_1)\theta(x_1 - mx_2)C_{\alpha\beta\mu\nu}, \tag{5}$$

where the $\{C_{\alpha\beta\mu\nu}\}$ are the ordinary (position-independent) elastic constants of the medium constituting the wedge, and $\theta(x)$ is the Heaviside unit step function

$$\theta(x) = 1 \quad x \geq 0$$
$$= 0 \quad x < 0. \tag{6}$$

It follows, therefore, that

$$\frac{\partial}{\partial x_1} C_{\alpha\beta\mu\nu}(\vec{x}) = [-m\delta(x_2 - mx_1)\theta(x_1 - mx_2) + \delta(x_1 - mx_2)\theta(x_2 - mx_1)]C_{\alpha\beta\mu\nu}, \tag{7a}$$

$$\frac{\partial}{\partial x_2} C_{\alpha\beta\mu\nu}(\vec{x}) = [\delta(x_2 - mx_1)\theta(x_1 - mx_2) - m\delta(x_1 - mx_2)\theta(x_2 - mx_1)]C_{\alpha\beta\mu\nu}, \tag{7b}$$

$$\frac{\partial}{\partial x_3} C_{\alpha\beta\mu\nu}(\vec{x}) = 0. \tag{7c}$$

If we specialize immediately to the case of a cubic crystal for which the cube axes coincide with the coordinate axes, and take note of Eqs. (7), we find that Eqs. (4) can be written explicitly as

$$\rho\ddot{u}_1 = \frac{\partial C_{11}}{\partial x_1}\frac{\partial u_1}{\partial x_1} + \frac{\partial C_{44}}{\partial x_2}\frac{\partial u_1}{\partial x_2} + \frac{\partial C_{12}}{\partial x_1}\frac{\partial u_2}{\partial x_2} + \frac{\partial C_{44}}{\partial x_2}\frac{\partial u_2}{\partial x_1} + \frac{\partial C_{12}}{\partial x_1}\frac{\partial u_3}{\partial x_3} + C_{11}\frac{\partial^2 u_1}{\partial x_1^2} + C_{44}\frac{\partial^2 u_1}{\partial x_2^2} + C_{44}\frac{\partial^2 u_1}{\partial x_3^2} + (C_{12} + C_{44})\left(\frac{\partial^2 u_2}{\partial x_1 \partial x_2} + \frac{\partial^2 u_3}{\partial x_1 \partial x_3}\right), \tag{8a}$$

$$\rho\ddot{u}_2 = \frac{\partial C_{44}}{\partial x_1}\frac{\partial u_1}{\partial x_2} + \frac{\partial C_{12}}{\partial x_2}\frac{\partial u_1}{\partial x_1} + \frac{\partial C_{44}}{\partial x_1}\frac{\partial u_2}{\partial x_1} + \frac{\partial C_{11}}{\partial x_2}\frac{\partial u_2}{\partial x_2} + \frac{\partial C_{12}}{\partial x_2}\frac{\partial u_3}{\partial x_3} + C_{44}\frac{\partial^2 u_2}{\partial x_1^2} + C_{11}\frac{\partial^2 u_2}{\partial x_2^2} + C_{44}\frac{\partial^2 u_2}{\partial x_3^2} + (C_{12} + C_{44})\left(\frac{\partial^2 u_1}{\partial x_1 \partial x_2} + \frac{\partial^2 u_3}{\partial x_2 \partial x_3}\right), \tag{8b}$$

$$\rho\ddot{u}_3 = \frac{\partial C_{44}}{\partial x_1}\left(\frac{\partial u_1}{\partial x_3} + \frac{\partial u_3}{\partial x_1}\right) + \frac{\partial C_{44}}{\partial x_2}\left(\frac{\partial u_2}{\partial x_3} + \frac{\partial u_3}{\partial x_2}\right) + C_{44}\frac{\partial^2 u_3}{\partial x_1^2} + C_{44}\frac{\partial^2 u_3}{\partial x_2^2} + C_{11}\frac{\partial^2 u_3}{\partial x_3^2} + (C_{12} + C_{44})\left(\frac{\partial^2 u_1}{\partial x_1 \partial x_3} + \frac{\partial^2 u_2}{\partial x_2 \partial x_3}\right), \tag{8c}$$

where we have used the contracted, Voigt, notation for the elastic constants.

We now carry out the linear transformation

$$\xi = x_1 - mx_2, \tag{9a}$$

$$\eta = -mx_1 + x_2. \tag{9b}$$

This transformation maps the straight line $x_2 = \alpha x_1$ into the straight line

$$\eta = \frac{\alpha - m}{1 - \alpha m}\xi. \tag{10}$$

In particular, the line $x_2 = mx_1$ is mapped into the line $\eta = 0$, and the line $x_1 = mx_2$ is mapped into the line $\xi = 0$. Consequently, if we introduce a Cartesian $\xi\eta$ plane, the wedge defined by Eqs. (1)–(2) is mapped by Eq. (9) into the right-angle wedge defined by (see Fig. 2)

$$\xi \geq 0, \quad \eta \geq 0, \quad -\infty \leq x_3 \leq \infty. \tag{11}$$

With the aid of the relations

$$\frac{\partial}{\partial x_1} = \frac{\partial}{\partial \xi} - m\frac{\partial}{\partial \eta}, \quad \frac{\partial}{\partial x_2} = -m\frac{\partial}{\partial \xi} + \frac{\partial}{\partial \eta}, \tag{12}$$

$$\frac{\partial^2}{\partial x_1^2} = \frac{\partial^2}{\partial \xi^2} - 2m\frac{\partial^2}{\partial \xi \partial \eta} + m^2\frac{\partial^2}{\partial \eta^2}, \tag{13a}$$

$$\frac{\partial^2}{\partial x_1 \partial x_2} = -m\frac{\partial^2}{\partial \xi^2} + (1 + m^2)\frac{\partial^2}{\partial \xi \partial \eta} - m\frac{\partial^2}{\partial \eta^2}, \tag{13b}$$

$$\frac{\partial^2}{\partial x_2^2} = m^2\frac{\partial^2}{\partial \xi^2} - 2m\frac{\partial^2}{\partial \xi \partial \eta} + \frac{\partial^2}{\partial \eta^2}, \tag{13c}$$

Eqs. (8) are transformed into

$$\rho\ddot{\tilde{u}}_1 = C_{11}[-m\delta(\eta)+\delta(\xi)]\left(\frac{\partial}{\partial\xi}-m\frac{\partial}{\partial\eta}\right)\tilde{u}_1 + C_{44}[\delta(\eta)-m\delta(\xi)]\left(-m\frac{\partial}{\partial\xi}+\frac{\partial}{\partial\eta}\right)\tilde{u}_1$$
$$+C_{12}[-m\delta(\eta)+\delta(\xi)]\left(-m\frac{\partial}{\partial\xi}+\frac{\partial}{\partial\eta}\right)\tilde{u}_2 + C_{44}[\delta(\eta)-m\delta(\xi)]\left(\frac{\partial}{\partial\xi}-m\frac{\partial}{\partial\eta}\right)\tilde{u}_2 + C_{12}[-m\delta(\eta)+\delta(\xi)]\frac{\partial\tilde{u}_3}{\partial x_3}$$
$$+C_{11}\left(\frac{\partial^2}{\partial\xi^2}-2m\frac{\partial^2}{\partial\xi\partial\eta}+m^2\frac{\partial^2}{\partial\eta^2}\right)\tilde{u}_1 + C_{44}\left(m^2\frac{\partial^2}{\partial\xi^2}-2m\frac{\partial^2}{\partial\xi\partial\eta}+\frac{\partial^2}{\partial\eta^2}\right)\tilde{u}_1 + C_{44}\frac{\partial^2\tilde{u}_1}{\partial x_3^2}$$
$$+(C_{12}+C_{44})\left(-m\frac{\partial^2}{\partial\xi^2}+(1+m^2)\frac{\partial^2}{\partial\xi\partial\eta}-m\frac{\partial^2}{\partial\eta^2}\right)\tilde{u}_2 + (C_{12}+C_{44})\left(\frac{\partial}{\partial\xi}-m\frac{\partial}{\partial\eta}\right)\frac{\partial\tilde{u}_3}{\partial x_3}, \quad (14a)$$

$$\rho\ddot{\tilde{u}}_2 = C_{44}[-m\delta(\eta)+\delta(\xi)]\left(-m\frac{\partial}{\partial\xi}+\frac{\partial}{\partial\eta}\right)\tilde{u}_1 + C_{12}[\delta(\eta)-m\delta(\xi)]\left(\frac{\partial}{\partial\xi}-m\frac{\partial}{\partial\eta}\right)\tilde{u}_1$$
$$+C_{44}[-m\delta(\eta)+\delta(\xi)]\left(\frac{\partial}{\partial\xi}-m\frac{\partial}{\partial\eta}\right)\tilde{u}_2 + C_{11}[\delta(\eta)-m\delta(\xi)]\left(-m\frac{\partial}{\partial\xi}+\frac{\partial}{\partial\eta}\right)\tilde{u}_2 + C_{12}[\delta(\eta)-m\delta(\xi)]\frac{\partial\tilde{u}_3}{\partial x_3}$$
$$+(C_{12}+C_{44})\left(-m\frac{\partial^2}{\partial\xi^2}+(1+m^2)\frac{\partial^2}{\partial\xi\partial\eta}-m\frac{\partial^2}{\partial\eta^2}\right)\tilde{u}_1 + C_{44}\left(\frac{\partial^2}{\partial\xi^2}-2m\frac{\partial^2}{\partial\xi\partial\eta}+m^2\frac{\partial^2}{\partial\eta^2}\right)\tilde{u}_2$$
$$+C_{11}\left(m^2\frac{\partial^2}{\partial\xi^2}-2m\frac{\partial^2}{\partial\xi\partial\eta}+\frac{\partial^2}{\partial\eta^2}\right)\tilde{u}_2 + C_{44}\frac{\partial^2\tilde{u}_2}{\partial x_3^2} + (C_{12}+C_{44})\left(-m\frac{\partial}{\partial\xi}+\frac{\partial}{\partial\eta}\right)\frac{\partial\tilde{u}_3}{\partial x_3}, \quad (14b)$$

$$\rho\ddot{\tilde{u}}_3 = C_{44}[-m\delta(\eta)+\delta(\xi)]\frac{\partial\tilde{u}_1}{\partial x_3} + C_{44}[\delta(\eta)-m\delta(\xi)]\frac{\partial\tilde{u}_2}{\partial x_3} + C_{44}[-m\delta(\eta)+\delta(\xi)]\left(\frac{\partial}{\partial\xi}-m\frac{\partial}{\partial\eta}\right)\tilde{u}_3$$
$$+C_{44}[\delta(\eta)-m\delta(\xi)]\left(-m\frac{\partial}{\partial\xi}+\frac{\partial}{\partial\eta}\right)\tilde{u}_3 + (C_{12}+C_{44})\left(\frac{\partial}{\partial\xi}-m\frac{\partial}{\partial\eta}\right)\frac{\partial\tilde{u}_1}{\partial x_3} + (C_{12}+C_{44})\left(-m\frac{\partial}{\partial\xi}+\frac{\partial}{\partial\eta}\right)\frac{\partial\tilde{u}_2}{\partial x_3}$$
$$+C_{44}\left(\frac{\partial^2}{\partial\xi^2}-2m\frac{\partial^2}{\partial\xi\partial\eta}+m^2\frac{\partial^2}{\partial\eta^2}\right)\tilde{u}_3 + C_{44}\left(m^2\frac{\partial^2}{\partial\xi^2}-2m\frac{\partial^2}{\partial\xi\partial\eta}+\frac{\partial^2}{\partial\eta^2}\right)\tilde{u}_3 + C_{11}\frac{\partial^2\tilde{u}_3}{\partial x_3^2}, \quad (14c)$$

where we have set

$$u_\alpha(x_1,\ x_2,\ x_3) = \tilde{u}_\alpha(\xi,\ \eta,\ x_3). \quad (15)$$

In Eqs. (14) it must be understood that $\xi \geq 0$ and $\eta \geq 0$.

Because the wedge is invariant against an arbitrary displacement parallel to the edge (i.e., parallel to the x_3 axis), we seek solutions of Eq. (14) of the form

$$\tilde{u}_\alpha(\xi,\ \eta,\ x_3) = \bar{u}_\alpha(\xi,\ \eta)\, e^{iqx_3 - i\omega t}. \quad (16)$$

When Eq. (16) is substituted into Eqs. (14) we find that the equations satisfied by the amplitude functions $\{\bar{u}_\alpha(\xi,\ \eta)\}$ are

$$-\rho\omega^2\bar{u}_1 = C_{11}[-m\delta(\eta)+\delta(\xi)]\left(\frac{\partial}{\partial\xi}-m\frac{\partial}{\partial\eta}\right)\bar{u}_1 + C_{44}[\delta(\eta)-m\delta(\xi)]\left(-m\frac{\partial}{\partial\xi}+\frac{\partial}{\partial\eta}\right)\bar{u}_1$$
$$+C_{12}[-m\delta(\eta)+\delta(\xi)]\left(-m\frac{\partial}{\partial\xi}+\frac{\partial}{\partial\eta}\right)\bar{u}_2 + C_{44}[\delta(\eta)-m\delta(\xi)]\left(\frac{\partial}{\partial\xi}-m\frac{\partial}{\partial\eta}\right)\bar{u}_2 + iqC_{12}[-m\delta(\eta)+\delta(\xi)]\,\bar{u}_3$$
$$+C_{11}\left(\frac{\partial^2}{\partial\xi^2}-2m\frac{\partial^2}{\partial\xi\partial\eta}+m^2\frac{\partial^2}{\partial\eta^2}\right)\bar{u}_1 + C_{44}\left(m^2\frac{\partial^2}{\partial\xi^2}-2m\frac{\partial^2}{\partial\xi\partial\eta}+\frac{\partial^2}{\partial\eta^2}\right)\bar{u}_1 - q^2C_{44}\bar{u}_1$$
$$+(C_{12}+C_{44})\left(-m\frac{\partial^2}{\partial\xi^2}+(1+m^2)\frac{\partial^2}{\partial\xi\partial\eta}-m\frac{\partial^2}{\partial\eta^2}\right)\bar{u}_2 + iq(C_{12}+C_{44})\left(\frac{\partial}{\partial\xi}-m\frac{\partial}{\partial\eta}\right)\bar{u}_3, \quad (17a)$$

$$-\rho\omega^2\bar{u}_2 = C_{44}[-m\delta(\eta)+\delta(\xi)]\left(-m\frac{\partial}{\partial\xi}+\frac{\partial}{\partial\eta}\right)\bar{u}_1 + C_{12}[\delta(\eta)-m\delta(\xi)]\left(\frac{\partial}{\partial\xi}-m\frac{\partial}{\partial\eta}\right)\bar{u}_1$$
$$+C_{44}[-m\delta(\eta)+\delta(\xi)]\left(\frac{\partial}{\partial\xi}-m\frac{\partial}{\partial\eta}\right)\bar{u}_2 + C_{11}[\delta(\eta)-m\delta(\xi)]\left(-m\frac{\partial}{\partial\xi}+\frac{\partial}{\partial\eta}\right)\bar{u}_2 + iqC_{12}[\delta(\eta)-m\delta(\xi)]\,\bar{u}_3$$
$$+(C_{12}+C_{44})\left(-m\frac{\partial^2}{\partial\xi^2}+(1+m^2)\frac{\partial^2}{\partial\xi\partial\eta}-m\frac{\partial^2}{\partial\eta^2}\right)\bar{u}_1 + C_{44}\left(\frac{\partial^2}{\partial\xi^2}-2m\frac{\partial^2}{\partial\xi\partial\eta}+m^2\frac{\partial^2}{\partial\eta^2}\right)\bar{u}_2$$
$$+C_{11}\left(m^2\frac{\partial^2}{\partial\xi^2}-2m\frac{\partial^2}{\partial\xi\partial\eta}+\frac{\partial^2}{\partial\eta^2}\right)\bar{u}_2 - q^2C_{44}\bar{u}_2 + iq(C_{12}+C_{44})\left(-m\frac{\partial}{\partial\xi}+\frac{\partial}{\partial\eta}\right)\bar{u}_3, \quad (17b)$$

$$-\rho\omega^2\bar{u}_3 = iqC_{44}[-m\delta(\eta)+\delta(\xi)]\bar{u}_1 + iqC_{44}[\delta(\eta)-m\delta(\xi)]\bar{u}_2 + C_{44}[-m\delta(\eta)+\delta(\xi)]\left(\frac{\partial}{\partial\xi}-m\frac{\partial}{\partial\eta}\right)\bar{u}_3$$
$$+C_{44}[\delta(\eta)-m\delta(\xi)]\left(-m\frac{\partial}{\partial\xi}+\frac{\partial}{\partial\eta}\right)\bar{u}_3 + iq(C_{12}+C_{44})\left(\frac{\partial}{\partial\xi}-m\frac{\partial}{\partial\eta}\right)\bar{u}_1 + iq(C_{12}+C_{44})\left(-m\frac{\partial}{\partial\xi}+\frac{\partial}{\partial\eta}\right)\bar{u}_2$$
$$+C_{44}\left(\frac{\partial^2}{\partial\xi^2}-2m\frac{\partial^2}{\partial\xi\partial\eta}+m^2\frac{\partial^2}{\partial\eta^2}\right)\bar{u}_3 + C_{44}\left(m^2\frac{\partial^2}{\partial\xi^2}-2m\frac{\partial^2}{\partial\xi\partial\eta}+\frac{\partial^2}{\partial\eta^2}\right)\bar{u}_3 - q^2C_{11}\bar{u}_3\,. \quad (17c)$$

We finally introduce the changes of variables

$$\xi = x/q\,,\quad \eta = y/q\,, \quad (18)$$

and define new coefficient functions $\{\hat{u}_\alpha(x,\,y)\}$ by

$$\bar{u}_1(\xi,\,\eta)=\hat{u}_1(x,\,y);\quad \bar{u}_2(\xi,\,\eta)=\hat{u}_2(x,\,y);\quad i\bar{u}_3(\xi,\,\eta)=\hat{u}_3(x,\,y)\,. \quad (19)$$

The purpose in making this last change in variables is to remove the dependence on the wave vector q from the right-hand side of the equations and to make the equations totally real. Thus, we obtain

$$-\rho\frac{\omega^2}{q^2}\hat{u}_1 = C_{11}[\delta(x)-m\delta(y)]\left(\frac{\partial}{\partial x}-m\frac{\partial}{\partial y}\right)\hat{u}_1 + C_{44}[-m\delta(x)+\delta(y)]\left(-m\frac{\partial}{\partial x}+\frac{\partial}{\partial y}\right)\hat{u}_1$$
$$+C_{12}[\delta(x)-m\delta(y)]\left(-m\frac{\partial}{\partial x}+\frac{\partial}{\partial y}\right)\hat{u}_2 + C_{44}[-m\delta(x)+\delta(y)]\left(\frac{\partial}{\partial x}-m\frac{\partial}{\partial y}\right)\hat{u}_2 + C_{12}[\delta(x)-m\delta(y)]\hat{u}_3$$
$$+C_{11}\left(\frac{\partial^2}{\partial x^2}-2m\frac{\partial^2}{\partial x\partial y}+m^2\frac{\partial^2}{\partial y^2}\right)\hat{u}_1 + C_{44}\left(m^2\frac{\partial^2}{\partial x^2}-2m\frac{\partial^2}{\partial x\partial y}+\frac{\partial^2}{\partial y^2}\right)\hat{u}_1 - C_{44}\hat{u}_1$$
$$+(C_{12}+C_{44})\left(-m\frac{\partial^2}{\partial x^2}+(1+m^2)\frac{\partial^2}{\partial x\partial y}-m\frac{\partial^2}{\partial y^2}\right)\hat{u}_2 + (C_{12}+C_{44})\left(\frac{\partial}{\partial x}-m\frac{\partial}{\partial y}\right)\hat{u}_3\,, \quad (20a)$$

$$-\rho\frac{\omega^2}{q^2}\hat{u}_2 = C_{44}[\delta(x)-m\delta(y)]\left(-m\frac{\partial}{\partial x}+\frac{\partial}{\partial y}\right)\hat{u}_1 + C_{12}[-m\delta(x)+\delta(y)]\left(\frac{\partial}{\partial x}-m\frac{\partial}{\partial y}\right)\hat{u}_1$$
$$+C_{44}[\delta(x)-m\delta(y)]\left(\frac{\partial}{\partial x}-m\frac{\partial}{\partial y}\right)\hat{u}_2 + C_{11}[-m\delta(x)+\delta(y)]\left(-m\frac{\partial}{\partial x}+\frac{\partial}{\partial y}\right)\hat{u}_2 + C_{12}[-m\delta(x)+\delta(y)]\hat{u}_3$$
$$+(C_{12}+C_{44})\left(-m\frac{\partial^2}{\partial x^2}+(1+m^2)\frac{\partial^2}{\partial x\partial y}-m\frac{\partial^2}{\partial y^2}\right)\hat{u}_1 + C_{44}\left(\frac{\partial^2}{\partial x^2}-2m\frac{\partial^2}{\partial x\partial y}+m^2\frac{\partial^2}{\partial y^2}\right)\hat{u}_2$$
$$+C_{11}\left(m^2\frac{\partial^2}{\partial x^2}-2m\frac{\partial^2}{\partial x\partial y}+\frac{\partial^2}{\partial y^2}\right)\hat{u}_2 - C_{44}\hat{u}_2 + (C_{12}+C_{44})\left(-m\frac{\partial}{\partial x}+\frac{\partial}{\partial y}\right)\hat{u}_3\,, \quad (20b)$$

$$-\rho\frac{\omega^2}{q^2}\hat{u}_3 = -C_{44}[\delta(x)-m\delta(y)]\hat{u}_1 - C_{44}[m\delta(x)+\delta(y)]\hat{u}_2 + C_{44}[\delta(x)-m\delta(y)]\left(\frac{\partial}{\partial x}-m\frac{\partial}{\partial y}\right)\hat{u}_3$$
$$+C_{44}[-m\delta(x)+\delta(y)]\left(-m\frac{\partial}{\partial x}+\frac{\partial}{\partial y}\right)\hat{u}_3 - (C_{12}+C_{44})\left(\frac{\partial}{\partial x}-m\frac{\partial}{\partial y}\right)\hat{u}_1 - (C_{12}+C_{44})\left(-m\frac{\partial}{\partial x}+\frac{\partial}{\partial y}\right)\hat{u}_2$$
$$+C_{44}\left(\frac{\partial^2}{\partial x^2}-2m\frac{\partial^2}{\partial x\partial y}+m^2\frac{\partial^2}{\partial y^2}\right)\hat{u}_3 + C_{44}\left(m^2\frac{\partial^2}{\partial x^2}-2m\frac{\partial^2}{\partial x\partial y}+\frac{\partial^2}{\partial y^2}\right)\hat{u}_3 - C_{11}\hat{u}_3\,. \quad (20c)$$

From these equations ω is seen to be linear in q.

To solve this system of equations we expand $\hat{u}_\alpha(x,\,y)$ as

$$\hat{u}_\alpha(x,\,y)=\sum_{k=0}^{\infty}\sum_{l=0}^{\infty}a_{kl}^{(\alpha)}\varphi_k(x)\varphi_l(y)\,, \quad (21)$$

where

$$\varphi_k(x)=|k\rangle=e^{-x/2}L_k(x)/k!\,, \quad (22)$$

and $L_k(x)$ is the kth Laguerre polynomial. The functions $\{\varphi_k(x)\}$ are orthonormal and complete in the interval $0\le x\le\infty$, and the presence of the factor $e^{-x/2}$ in their definition is convenient, since we are looking for displacement amplitudes localized in the vicinity of the apex of the wedge. Various properties of the functions $\{\varphi_k(x)\}$ which are useful for the present calculations are presented in Ref. 1.

When the expansion (21) is substituted in Eqs. (20), and the orthonormality of the $\{\varphi_k(x)\}$ is used, the resulting equations for the expansion coefficients $\{a_{kl}^{(\alpha)}\}$ can be written in the form

$$\Omega^2 a_{ij}^{(\alpha)}=\sum_{\beta=1}^{3}\sum_{k,\,l}A_{ij;kl}^{(\alpha\beta)}(m)\,a_{kl}^{(\beta)}\,,\quad \alpha=1,\,2,\,3\,, \quad (23)$$

where

$$\Omega^2=\rho\omega^2/C_{44}q^2\,. \quad (24)$$

From Eq. (24) we see that Ω is the speed of propagation of the edge mode in units such that the value $\Omega = 1.0$ corresponds to the speed of the bulk transverse acoustic mode in the (100) direction. The matrix elements $\{A^{(\alpha\beta)}_{ij;kl}(m)\}$ are given by

$$A^{(11)}_{ij;kl}(m) = \{\tfrac{1}{4}(3-A)\delta_{ik}\delta_{jl} + A\delta_{jl}[\min(i,\ k)+\tfrac{1}{2}] + \delta_{ik}[\min(j,\ l)+\tfrac{1}{2}]\}$$
$$+ m(A+1)\{-[\tfrac{1}{2}\delta_{ik}+\theta(k-i-1)] - [\tfrac{1}{2}\delta_{jl}+\theta(l-j-1)] + 2[\tfrac{1}{2}\delta_{ik}+\theta(k-i-1)][\tfrac{1}{2}\delta_{jl}+\theta(l-j-1)]\}$$
$$+ m^2\{-\tfrac{1}{4}(A+1)\delta_{ik}\delta_{jl} + A\delta_{ik}[\min(l,\ j)+\tfrac{1}{2}] + \delta_{jl}[\min(i,\ k)+\tfrac{1}{2}]\}, \quad (25a)$$

$$A^{(12)}_{ij;kl}(m) = \{B[\tfrac{1}{2}\delta_{jl}+\theta(l-j-1)] + [\tfrac{1}{2}\delta_{ik}+\theta(k-i-1)] - (B+1)[\tfrac{1}{2}\delta_{ik}+\theta(k-i-1)][\tfrac{1}{2}\delta_{jl}+\theta(l-j-1)]\}$$
$$+ m(B+1)\{-\delta_{kl}(k+\tfrac{1}{2}) - \delta_{ik}(l+\tfrac{1}{2}) + \delta_{ik}[\tfrac{1}{4}\delta_{jl} + (l-j)\theta(l-j-1)] + \delta_{jl}[\tfrac{1}{4}\delta_{ik} + (k-i)\theta(k-i-1)]\}$$
$$+ m^2\{B[\tfrac{1}{2}\delta_{ik}+\theta(k-i-1)] + [\tfrac{1}{2}\delta_{jl}+\theta(l-j-1)] - (B+1)[\tfrac{1}{2}\delta_{ik}+\theta(k-i-1)][\tfrac{1}{2}\delta_{jl}+\theta(l-j-1)]\}, \quad (25b)$$

$$A^{(13)}_{ij;kl}(m) = \delta_{jl}\{-B + (B+1)[\tfrac{1}{2}\delta_{ik}+\theta(k-i-1)]\} + m\delta_{ik}\{B - (B+1)[\tfrac{1}{2}\delta_{jl}+\theta(l-j-1)]\}, \quad (25c)$$

$$A^{(21)}_{ij;kl}(m) = A^{(12)}_{ji;lk}(m), \quad (25d)$$

$$A^{(22)}_{ij;kl}(m) = A^{(11)}_{ji;lk}(m), \quad (25e)$$

$$A^{(23)}_{ij;kl}(m) = A^{(13)}_{ji;lk}(m), \quad (25f)$$

$$A^{(31)}_{ij;kl}(m) = \delta_{jl}\{1 - (B+1)[\tfrac{1}{2}\delta_{ik}+\theta(k-i-1)]\} + m\delta_{ik}\{-1 + (B+1)[\tfrac{1}{2}\delta_{jl}+\theta(l-j-1)]\}, \quad (25g)$$

$$A^{(32)}_{ij;kl}(m) = A^{(31)}_{ji;lk}(m), \quad (25h)$$

$$A^{(33)}_{ij;kl}(m) = \{\delta_{ik}\delta_{jl}(A-\tfrac{1}{2}) + \delta_{ik}[\min(j,\ l)+\tfrac{1}{2}] + \delta_{jl}[\min(i,\ k)+\tfrac{1}{2}]\}$$
$$+ m\{-2[\tfrac{1}{2}\delta_{ik}+\theta(k-i-1)] - 2[\tfrac{1}{2}\delta_{jl}+\theta(l-j-1)] + 4[\tfrac{1}{2}\delta_{ik}+\theta(k-i-1)][\tfrac{1}{2}\delta_{jl}+\theta(l-j-1)]\}$$
$$+ m^2\{-\tfrac{1}{2}\delta_{ik}\delta_{jl} + \delta_{ik}[\min(j,\ l)+\tfrac{1}{2}] + \delta_{jl}[\min(i,\ k)+\tfrac{1}{2}]\}. \quad (25i)$$

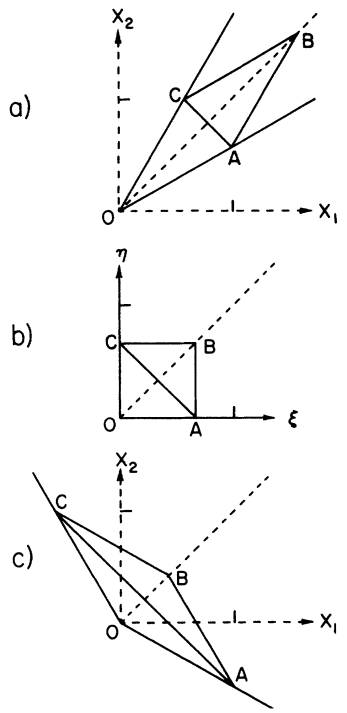

FIG. 2. Effect of the mapping Eqs. (9) upon an acute-angle wedge (a) and upon an obtuse-angle wedge (c) is shown in the $\eta\xi$ space (b). The line segments $OABC$ are equivalent in all three diagrams.

In writing these expressions we have used the notation

$$A = C_{11}/C_{44}, \quad B = C_{12}/C_{44}, \quad (26)$$

and

$$\theta(k) = 1, \quad k \geq 0$$
$$= 0, \quad k < 0. \quad (27)$$

For $m = 0$ the expressions given by Eqs. (25) coincide with those obtained in Ref. 1.

The matrix $A^{(\alpha\beta)}_{ij;kl}(m)$ is not symmetric, i.e.,

$$A^{(\alpha\beta)}_{ij;kl}(m) \neq A^{(\beta\alpha)}_{kl;ij}(m). \quad (28)$$

The wedge defined by Eqs. (1) and (2) is invariant under reflection in the plane $x_1 = x_2$ or, equivalently, in the interchange of x_1 and x_2. From Eqs. (9) we see that the interchange of x_1 and x_2 is equivalent to the interchange of ξ and η, and from Eq. (18) this is equivalent to the interchange of x and y. Thus, the wedge in the xy plane is invariant under the operations of the point group C_s, whose elements are E, the identity, and σ, reflection in the plane $x = y$. If we write Eqs. (20) in the form

$$-\rho\frac{\omega^2}{q^2}\hat{u}_\alpha(x,\ y) = \sum_\beta L_{\alpha\beta}(x,\ y)\hat{u}_\beta(x,\ y), \quad (29)$$

which defines the differential operators $\{L_{\alpha\beta}(x,\ y)\}$ implicitly, it can be shown straightforwardly that

these operators transform under the operations of the group C_s according to

$$L_{\alpha\beta}(\overleftrightarrow{S}\,\vec{x}_{\parallel}) = \sum_{\mu\nu} S_{\alpha\mu} S_{\beta\nu} L_{\mu\nu}(\vec{x}_{\parallel}) . \tag{30}$$

In Eq. (30) $\overleftrightarrow{S}$ is the 3×3 real, orthogonal matrix representation of an operation of the group C_s, and $\vec{x}_{\parallel}$ is the vector $(x, y, 0)$. On the basis of the result given by Eq. (30) we can immediately conclude, using the same arguments as were employed in Ref. 1, that the displacement fields belonging to the two irreducible representations Γ_1 and Γ_2 of the group C_s possess the properties

$$\begin{aligned}
&\Gamma_1\text{: } \hat{u}_1(y, x) = \hat{u}_2(x, y), \quad \Gamma_2\text{: } \hat{u}_1(y, x) = -\hat{u}_2(x, y) ,\\
&\hat{u}_2(y, x) = \hat{u}_1(x, y), \qquad \hat{u}_2(y, x) = -\hat{u}_1(x, y) ,\\
&\hat{u}_3(y, x) = \hat{u}_3(x, y), \qquad \hat{u}_3(y, x) = -\hat{u}_3(x, y) .
\end{aligned} \tag{31}$$

These conditions translate into the following conditions on the coefficients $\{a_{ij}^{(\alpha)}\}$ in the expansions (21):

$$a_{ji}^{(1)} = \pm a_{ij}^{(2)}, \quad a_{ji}^{(2)} = \pm a_{ij}^{(1)}, \quad a_{ji}^{(3)} = \pm a_{ij}^{(3)} , \tag{32}$$

where the upper (lower) signs refer to displacements belonging to Γ_1 (Γ_2).

Equations (32) were used to simplify the eigenvalue problem (23). The equations which were solved in the present work are

$$\begin{aligned}
\Omega^2 a_{ij}^{(1)} &= \sum_{kl} \{B_{ij;kl}^{(11)}(m) a_{kl}^{(1)} + B_{ij;kl}^{(13)}(m) a_{kl}^{(3)}\} ,\\
\Omega^2 a_{ij}^{(3)} &= \sum_{kl} \{B_{ij;kl}^{(31)}(m) a_{kl}^{(1)} + B_{ij;kl}^{(33)}(m) a_{kl}^{(3)}\} ,
\end{aligned} \tag{33}$$

and $a_{ij}^{(2)}$ was obtained from $a_{ij}^{(1)}$ by means of Eqs. (32). The matrix elements $\{B_{ij;kl}^{(\alpha\beta)}(m)\}$ appearing in Eqs. (33) are

$$\begin{aligned}
B_{ij;kl}^{(11)}(m) &= A_{ij;kl}^{(11)}(m) \pm A_{ij;lk}^{(12)}(m) ,\\
B_{ij;kl}^{(13)}(m) &= \tfrac{1}{2}[A_{ij;kl}^{(13)}(m) \pm A_{ij;lk}^{(13)}(m)] ,\\
B_{ij;kl}^{(31)}(m) &= A_{ij;kl}^{(31)}(m) \pm A_{ij;lk}^{(32)}(m) ,\\
B_{ij;kl}^{(33)}(m) &= \tfrac{1}{2}[A_{ij;kl}^{(33)}(m) \pm A_{ij;lk}^{(33)}(m)] ,
\end{aligned} \tag{34}$$

where, again, the upper (lower) signs refer to modes having Γ_1 (Γ_2) symmetry.

In addition to making it possible to solve for the frequencies of modes of definite symmetry, the use of Eqs. (33)–(34) in place of Eq. (23) results in the reduction in the dimensionality of the matrices to be diagonalized by a factor of one-third, for the same number of terms in the expansions (21).

III. RESULTS

We have solved the set of Eqs. (33)–(34) by using standard eigenvalue subroutines for nonsymmetric matrices. The size of the matrix is determined by the number of terms kept in the expansion Eq. (21). For these calculations, all terms were retained that satisfied the condition $k+l \le p$. For a given value of the integer p, the dimensionality of the matrix to be diagonalized is $(p+1)(p+2) \times (p+1)(p+2)$. Even though the matrix is not symmetric, all of the eigenvalues were real for all cases studied. For most of the calculations, the parameters A and B were given the values of 3.0 and 1.0, respectively. This is the case for which the elastic constants simultaneously satisfy the isotropy condition $C_{11} - C_{12} = 2C_{44}$, and the Cauchy relation $C_{12} = C_{44}$. For these values of A and B, the value of Ω^2 corresponding to Rayleigh surface waves is $\Omega_R^2 = 2 - \frac{2}{3}\sqrt{3} = 0.845\,299$.[4] The value $\Omega^2 = 1.0$ corresponds to bulk transverse acoustic waves.

In Fig. 3 we show the lowest ten eigenvalues as functions of the integer p for a wedge whose apex angle $\theta = 45°$. The value of Ω^2 corresponding to Rayleigh surface waves, Ω_R^2, is shown by a dotted line. For the two modes whose frequencies fall well below the Rayleigh value, the displacement patterns are localized near the edge, and both are termed vibrational edge modes. The eigenvalues that fall below the Rayleigh value show good convergence for values of $p = 10$. This good convergence of the lowest eigenvalues was found to hold for all apex angles between 30° and 180°. It is of particular interest to note that the frequencies of modes having Γ_1 and Γ_2 symmetry for a wedge whose apex angle is 45° are not interleaved, as is the case for a right-angled wedge reported earlier.[1]

Those modes whose eigenvalues are larger than the Rayleigh value cannot be considered as corresponding to real normal modes of the wedge. This is because the expansion of the displacements in

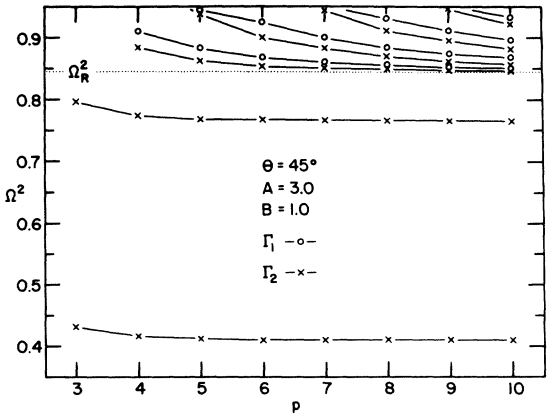

FIG. 3. Plot of the convergence of the lowest eigenvalues as a function of the integer p for a wedge of angle $\theta = 45°$. Ω_R^2 is the eigenvalue appropriate to Rayleigh surface modes.

Eq. (21) implicitly contains a decaying exponential. Hence, the sums in Eq. (21) must contain an infinite number of terms to represent either surface or bulk acoustic phonons, since these extend an infinite distance away from the apex of the wedge. For this reason, the calculation of the eigenvalues for these modes does not converge as it does for the lower-frequency modes. However, a variational principle applies to this calculation,[1] and the eigenvalues for these higher-frequency modes are upper limits to the actual values. Thus the modes in Fig. 3 (and in Figs. 4 and 5) whose eigenvalue falls above the Rayleigh value should be considered as artifacts of the calculation. The situation here is analogous to that encountered in solving for Rayleigh surface waves on a semi-infinite medium wherein one obtains a cubic equation for the square of the frequency. One of the three solutions corresponds to a speed smaller than the transverse acoustic bulk phonon speed, and can be shown to be related to a real, positive decay constant (the Rayleigh solution). The other two solutions, however, correspond to speeds greater than the transverse acoustic bulk phonon speed and have decay constants that are imaginary. Thus, they do not represent modes that are localized near the surface, and are ignored in the context of the theory of Rayleigh waves.

In Fig. 4 we show the lowest-frequency Γ_2 modes as functions of the wedge angle θ. For small angles, the convergence is not as rapid as seen in Fig. 3, and a value of $p = 12$ was used for the angles $\theta = 20^\circ$ and 25°. For angles below 20°, the eigenvalues were estimated by visual extrapolation of the curve of eigenvalue versus integer p. Therefore, these eigenvalues should be considered as approximate. Attempts were made to extrapolate the curves of eigenvalues as a function of integer p in a more quantitative way by fitting the last few points to a series in inverse powers of p. These attempts were abandoned since (a) not all eigenvalues seem to have the same convergence properties, and (b) the extrapolated value by this method was often greater than the eigenvalue calculated for the largest value of p instead of smaller. A change in the formalism which could possibly lead to faster convergence would be to replace the characteristic length of q^{-1} in Eq. (18) by aq^{-1}, where a is an adjustable parameter of the order of unity. Then, by manipulation of the parameter a, one should be able to change the convergence rate of the eigenvalues by adjusting the rate of decay of the lowest-order Laguerre functions to approximate more closely the actual displacement pattern.

All of the modes whose eigenvalues fall below the Rayleigh value, for value of θ smaller than 105°, are of Γ_2 symmetry (shown in Fig. 4). They correspond to the antisymmetric flexural (asf)

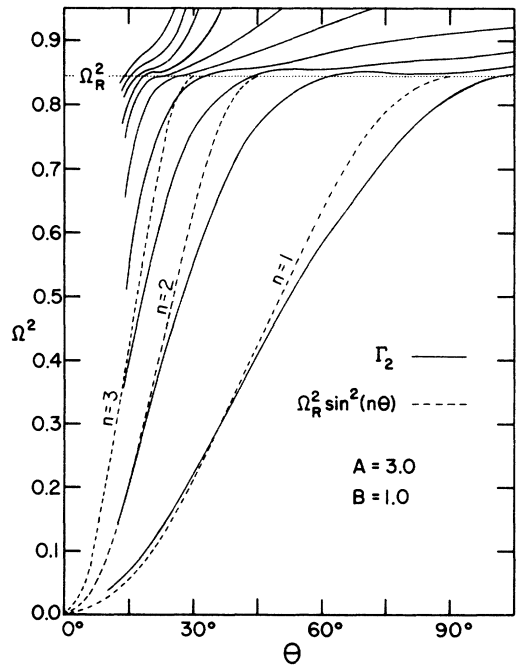

FIG. 4. Eigenvalues of the Γ_2 symmetry modes as functions of the wedge angle θ. Also shown is the empirical dependence $\Omega^2 = \Omega_R^2 \sin^2 n\theta$ suggested by Lagasse *et al.*

modes described by Lagasse, Mason, and Ash.[2] As the angle of the wedge decreases, the number of these Γ_2 modes with frequencies below the Rayleigh value increases dramatically. This result has also been obtained by Lagasse, Mason, and Ash.[2] The fact that a large number of localized modes exist for very thin wedges is to be expected. This is because as the wedge angle becomes very small, the wedge modes become similar to the vibrational modes localized near the end of a very thin ridge whose cross section is rectangular. It has been experimentally verified that these ridge waveguides become heavily overmoded as the ratio of the ridge height to ridge width becomes large.[2]

A physical explanation for the large number of edge modes of Γ_2 symmetry for small values of θ seems to be that very thin wedges (and ridges) are much more flexible than wedges of large apex angle, and can therefore vibrate in a greater number of localized modes, characterized by more nodal lines parallel to the x_3 axis in the midplane of the wedge. The thinner the wedge the more flexible it is in a Γ_2 mode, in which the two faces move in the same direction, and the more vibrational modes it can sustain.

Also shown in Fig. 4 is the empirical dependence of the eigenvalue upon wedge angle suggested by Lagasse *et al.* In terms of the eigenvalue, this dependence is given by

$$\Omega^2/\Omega_R^2 = \sin^2 n\theta, \quad n = 1, 2, 3, \ldots \ (n\theta < 90^\circ). \quad (35)$$

We see that the actual eigenvalues fall somewhat below those given by Eq. (35). In particular, this expression becomes quite inaccurate for any but the lowest values of n.

In Fig. 5 we show, on an expanded eigenvalue scale, all modes whose eigenvalue falls between 0.80 and 0.90 for wedge angles between 0° and 180°. It is of particular interest to note that a single mode of Γ_1 symmetry in the region of $\theta = 150°$ has an eigenvalue below the Rayleigh value. As the wedge angle θ increases to 180°, the eigenvalue of this mode becomes equal to the Rayleigh value. For all wedge angles below ~125°, all Γ_1 modes have eigenvalues above the Rayleigh value. This appears to be true even as the angle θ goes to 0°. We closely investigated these solutions to see whether or not the eigenvalue for these Γ_1 modes actually does rise above the Rayleigh value as the angle θ decreases. When Ω is greater than Ω_R, the series solution does not properly converge due to the fact that the basis set chosen is only appropriate for modes that are localized. To be sure that these mode frequencies do in fact fall above the Rayleigh value and are not merely consequences of our use of too few terms in the assumed series solution, we examined the eigenvectors corresponding to these modes to determine which terms in the series are the most important. For the modes whose eigenvalues were below the Rayleigh value, the first terms in the series corresponding to the lowest orders of the Laguerre functions were the dominant contributions to the solution. When the eigenvalue was above the Rayleigh value, however, it was the higher-order Laguerre functions which made the dominant contributions to the solutions. Hence we conclude that the Γ_1 mode frequencies do in fact fall above the Rayleigh value for wedge angles smaller than ~125°, but that the eigenvalues given in Fig. 5 are only upper limits. Also of interest in Fig. 5 is the fact that for wedge angles θ between ~100° and ~125° there are no modes with eigenvalues below the Rayleigh value, which implies there are no vibrational edge modes of either symmetry for this range of wedge angles.

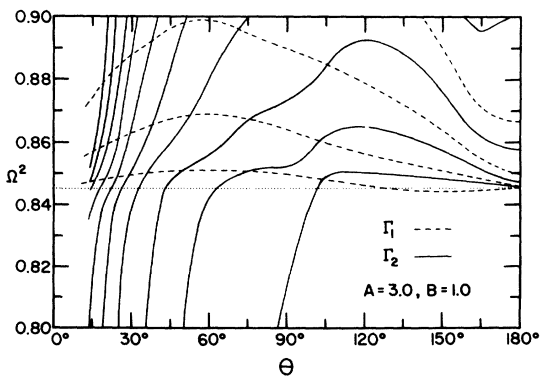

FIG. 5. All of the eigenvalues, on an expended scale, as functions of the wedge angle θ. Between $\theta = 100°$ and 125°, there are no vibrational edge modes for this choice of the elastic constant parameters A and B.

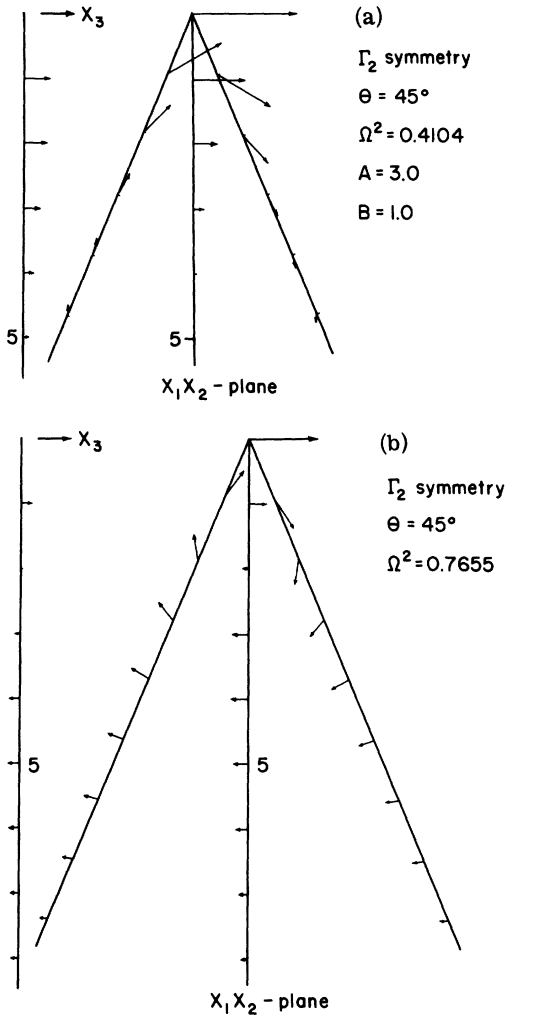

FIG. 6. (a) Displacement pattern of the lowest eigenvalue Γ_2 symmetry vibrational edge mode for a wedge of angle $\theta = 45°$. The x_3 displacements are those occurring at the surface of the wedge and are 90° out of phase with the displacements in the x_1x_2 plane. The x_3 displacements along the midplane of the wedge are identically zero. The unit of length is q^{-1}. (b) Displacement pattern for the second-lowest eigenvalue Γ_2 symmetry vibrational edge mode.

The displacement pattern corresponding to any mode is found by solving for the eigenvector in Eq. (33). Using Eq. (21), the set of displacements $\{\hat{u}_\alpha(x, y)\}$ in the mapped unitless space (x, y) defined in Eqs. (18) and (19) are found. These dis-

placements are then converted to the set of real space displacements $\{u_\alpha(x_1, x_2)\}$ by performing the inverse of the transformation in Eq. (19). It is important to notice that due to the introduction of an i into Eq. (19), the x_3 component of the displacements is 90° out of phase with the displacements in the x_1x_2 plane.

In Fig. 6 we show the x_1x_2 displacement pattern for the two Γ_2 symmetry vibrational edge modes for a wedge angle $\theta = 45°$, which are calculated using a value of $p = 10$. The displacements in the x_3 direction for one of the surfaces of the wedge are also shown. We note that the x_3 displacements for the other surface of the wedge are the negatives of those shown, and that the x_3 displacements along the midplane of the wedge are identically zero for modes of this symmetry. As expected, the lower-frequency mode is more localized near the apex of the wedge than the higher-frequency mode. Since the unit of length is q^{-1}, we see that the edge modes are confined to be within a few wavelengths of the apex of the wedge.

In Fig. 7 we show the displacement pattern for the Γ_1 symmetry vibrational edge mode for a wedge of angle $\theta = 150°$, again calculated for a value of $p = 10$. This mode is strongly localized near the two surfaces of the wedge, but is only weakly localized near the apex. Since the mode is of Γ_1 symmetry, the x_3 displacements at both surfaces are in the same direction. The x_3 displacements along the midplane for this symmetry mode are not zero, but are rather 180° out of phase with the x_3 displacements at the surfaces.

Finally, in Fig. 8 we show the change in the eigenvalue, $\Delta\Omega^2$, for a wedge of angle $\theta = 45°$ as a function of the change in the ratio of the elastic constant parameters A/B. The elastic constants are varied such that the isotropy condition is always satisfied. Only the Cauchy relation is violated when changing A/B. Of interest is the result that the group of six eigenvalues of mixed symmetry that fall slightly above the Rayleigh value have a very similar dependence on A/B with one another, and with the Rayleigh value, and that this dependence is different from that of the two vibrational edge modes whose eigenvalues fall below the Rayleigh value. In particular, the eigenvalue of the strongly localized vibrational edge mode is very nearly independent of the change in the elastic constants.

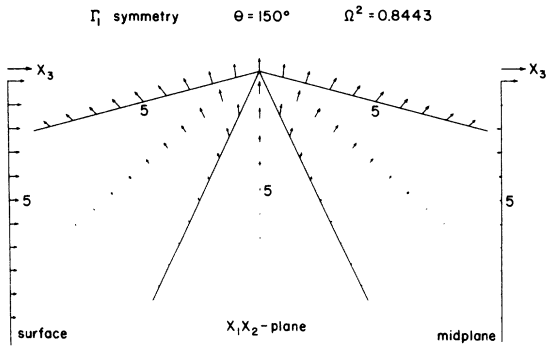

FIG. 7. Displacement pattern of the Γ_1 symmetry vibrational edge mode for a wedge of angle $\theta = 150°$. The x_3 displacements at both surfaces are the same and are 90° out of phase with the displacements in the x_1x_2 plane. The x_3 displacements along the midplane are also shown.

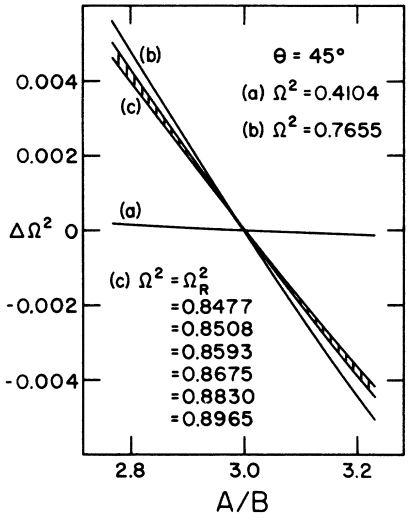

FIG. 8. Change in the eigenvalues $\Delta\Omega^2$ with the elastic constant parameter ratio A/B for eight of the lowest eigenvalues of a wedge of angle $\theta = 45°$ and for the eigenvalue appropriate to Rayleigh surface waves. $\Delta\Omega^2$ is defined such that it is identically zero for each mode when the ratio of $A/B = 3.0$. The dependence of the two vibrational edge modes is quantitatively different from the dependence of the modes whose eigenvalues are above the Rayleigh value.

IV. CONCLUSIONS

We have found the following.

(i) All vibrational edge modes for wedges of apex angle θ less than 100° are of Γ_2 symmetry (antisymmetric flexural modes).

(ii) The number of vibrational edge modes localized near the apex of a wedge increases as the wedge angle decreases.

(iii) For wedge angles θ between 125° and 180° there is a single vibrational edge mode of Γ_1 symmetry. The eigenvalue of this mode is very close to the Rayleigh value, and this mode is not strongly localized near the apex of the wedge.

(iv) There is a range of values of the wedge angle θ for which no vibrational edge modes exist. For the case of an isotropic medium satisfying the Cauchy relation, this range of θ values is between 100° and 125°. This range may vary somewhat as

the elastic constants are changed.

(v) The degree of localization of the displacements near the apex of the wedge for a given mode increases as the eigenvalue for that mode decreases in magnitude from the Rayleigh value.

(vi) In the method we have presented there are no mathematical approximations in setting up the eigenvalue problem. The accuracy of the results is dependent only upon the number of terms retained in the double expansion of the displacement amplitudes. The numerical results we obtain for the lowest eigenvalue, agree very well with results obtained recently by Lagasse[5] using the method of Lagasse *et al.*[2] for the choice of elastic constants corresponding to $A = 3.0$ and $B = 1.0$.

The results presented in this paper, and the theory underlying them, have been obtained on the assumption that the elastic medium being considered is not piezoelectric. The extension of the present theory of edge modes to piezoelectric solids would be of interest due to the technological utility of such materials. We are now exploring this problem.

ACKNOWLEDGMENT

We would like to thank T. M. Sharon for his work in examining the convergence properties of the Γ_1 modes.

---

*Research supported in part by the Air Force Office of Scientific Research, Office of Aerospace Research, USAF, under Grant No. AFOSR 71-2018.

†Research supported by the Office of Naval Research under Contract No. N00014-69-A-0200-9003.

[1]A. A. Maradudin, R. F. Wallis, D. L. Mills, and R. L. Ballard, Phys. Rev. B 6, 1106 (1972).

[2]P. E. Lagasse, I. M. Mason, and E. A. Ash, IEEE Trans. Microwave Theory Tech. (to be published). See in addition: P. E. Lagasse and I. M. Mason, Electron. Lett. 8, 82 (1972); I. M. Mason, R. M. De La Rue, R. V. Schmidt, and E. A. Ash, Electron. Lett. 7, 395 (1971).

[3]L. Dobrzynski and A. A. Maradudin, Phys. Rev. B 6, 3810 (1972).

[4]A. E. H. Love, *A Treatise on the Mathematical Theory of Elasticity* (Dover Publications, New York, 1944), pp. 307–309.

[5]P. E. Lagasse (private communication). See in addition: P. E. Lagasse, Electron. Lett. 8, 372 (1972).